Analysis of the Shielding Effectiveness of Metallic Enclosures Excited by Internal Sources Through an Efficient Method of Moment Approach

Rodolfo Araneo and Giampiero Lovat

Department of Electrical Engineering
"Sapienza" University of Rome, Via Eudossiana 18, 00184 Roma, Italy
rodolfo.araneo@uniroma1.it, giampiero.lovat@uniroma1.it

***Abstract*—** The shielding effectiveness of rectangular metallic enclosures having thin or thick apertures in one of their walls and possibly loaded with conducting bodies is studied in detail for internal electromagnetic sources consisting of electric or magnetic dipoles. The analysis is performed through an efficient integral-equation formulation based on the Method of Moments, which makes use of several numerical tools (acceleration of the enclosure Green's function evaluation, its interpolation, possible use of entire-domain basis functions, etc...) and physically-based approximations, critically discussed. Several cases are studied and comparisons with results obtained through different full-wave commercial software confirm the accuracy of the proposed approach and its superior performance in terms of computational time and memory storage.

***Index Terms*—** Shielding effectiveness (SE), enclosures, apertures, method of moments (MoM).

I. INTRODUCTION

The analysis of the interaction between an electromagnetic (EM) field and a metallic enclosure is a classical problem in EM shielding. The metallic cavity is usually adopted to shield the interior components from external EM radiators or vice versa, to protect the external environment from the radiation caused by interior EM sources. In any case, the role of the metallic enclosure is that of reducing the EM interference between the inner and the outer world. In this connection, the most important coupling mechanism occurs through the unavoidable presence of apertures on the enclosure walls (which are necessary for many practical purposes) [1].

A metallic enclosure behaves effectively as a resonant EM system, i.e., close to certain characteristic (resonant) frequencies the field amplitude can become very large (ideally infinite for perfectly conducting (PEC) walls). In the presence of apertures, the structure still remains resonant although the resonant frequencies can be shifted and the quality factor reduced (because of radiation losses through the apertures). In any case, at such resonant frequencies, the EM interference is maximum and the shielding effectiveness (SE) of the system dramatically deteriorates. The possible presence of internal loads is another crucial factor that influences the value of the resonant frequencies and the spatial distribution of the field [2]. Finally, the SE depends also on the considered EM source; the latter is usually taken as an impinging uniform plane wave, but, especially if radiation from the interior of the cavity is considered, it could be an electric or a magnetic finite source (e.g., a short-wire or a small-loop antenna) [3].

All these issues call for an efficient and reliable numerical tool for the EM analysis and many numerical techniques have been applied to this classical problem, e.g., analytical formulations [4-6], finite-element [7], mode-matching [8], method-of-moments [9-11], finite-difference-time-domain [12-14], and hybrid [15] approaches.

In this work, we adopt a standard integral-equation (IE) approach for the analysis of metallic enclosures with apertures of arbitrary shape and thickness and possibly loaded with 2-D or 3-D metallic objects. Contrarily to most of the studies (which assume an external plane-wave excitation), we consider here both electric and magnetic dipoles with arbitrary orientation as sources of the incident EM field. In fact, dipoles can represent

practical sources such as short-linear or small-loop antennas. The problem is solved through a mixed-potential formulation of the Method of Moments (MoM). Several numerical tools (such as acceleration of the enclosure Green's function (GF) evaluation, its interpolation, use of different basis functions) and physically-based approximations are introduced to increase the efficiency of the formulation. Finally, the results are compared with those obtained through different full-wave commercial software thus showing the accuracy of the proposed approach and its superior performance.

II. ELECTROMAGNETIC PROBLEM FORMULATION

The EM problem under analysis is sketched in Fig. 1, together with the adopted reference system and the involved geometrical parameters. A rectangular metallic cavity with PEC walls and dimensions $\ell_x \times \ell_y \times \ell_z$ is excited by either an electric or a magnetic dipole of unit amplitude and directed along the direction $\mathbf{u}_d$. The enclosure walls may have a finite thickness t, and one of them (e.g., that located at the plane $z = l_z$) may have one or more apertures of arbitrary shape. Finally, the enclosure can also contain PEC objects of arbitrary shape.

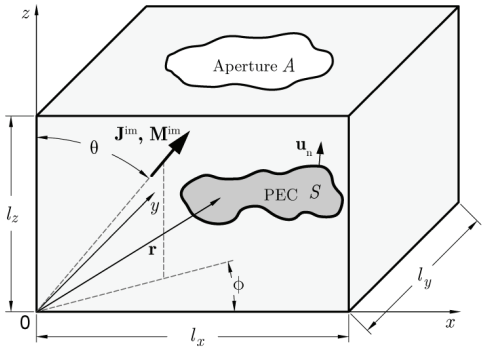

Fig. 1. Metallic rectangular enclosure (with an aperture on one of its walls and loaded with a conducting object) excited by arbitrarily directed electric and magnetic dipoles. The adopted reference system and the involved geometrical parameters are also shown.

In the absence of loading, the incident electric field $\mathbf{E}^{\text{inc}}$ is that radiated in free-space by the impressed dipole sources and it corresponds to a suitable combination (depending on the orientation of the dipoles) of the components of the free-space dyadic electric GFs ($\underline{\mathbf{G}}^{\text{fs}}_{\text{E,J/M}}$) (the subscripts J or M indicate an electric or a magnetic source, respectively). The electric shielding effectiveness SE_E of the enclosure at a given point $\mathbf{r}$ is thus defined as

$$\text{SE}_E = 20 \log \frac{\left|\mathbf{E}^{\text{inc}}(\mathbf{r})\right|}{\left|\mathbf{E}(\mathbf{r})\right|} \tag{1}$$

where $\mathbf{E}(\mathbf{r})$ is the electric field at $\mathbf{r}$ due to the radiating dipole sources in the presence of the enclosure, apertures, and conducting objects.

III. INTEGRAL-EQUATION APPROACH

The set of IEs which solve the problem can be derived through a customary application of the equivalence principle [1], as illustrated in Fig. 2: first, for finite-thickness walls, both interfaces of the aperture in $z = l_z$ (section A_i) and $z = l_z + t$ (section A_e) are short-circuited and equivalent magnetic current densities $\mathbf{M}_\text{i}$ and $\mathbf{M}_\text{e}$ are introduced on them. Next, an equivalent electric current density $\mathbf{J}$ is introduced over the surface S of the PEC load (which is then removed). The problem is thus decomposed into three-coupled problems: the metallic enclosure (region 1), the closed short-circuited aperture (region 2), and the external region (region 3).

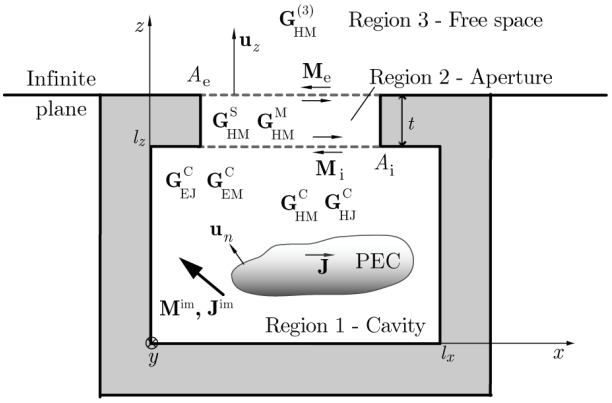

Fig. 2. Aperture in the thick conducting wall of the metallic enclosure and application of the equivalence principle.

By enforcing the boundary conditions at the sections A_i and A_e we have

$$\mathbf{u}_z \times \left[\mathbf{H}^{\mathrm{sc}}(\mathbf{r}) + \mathbf{H}^{-}(\mathbf{r}) \right] = \mathbf{u}_z \times \mathbf{H}^{+}(\mathbf{r}) \qquad \mathbf{r} \in A_\mathrm{i} \quad (2a)$$

$$\mathbf{u}_z \times \mathbf{H}^{-}(\mathbf{r}) = \mathbf{u}_z \times \mathbf{H}^{+}(\mathbf{r}) \qquad \mathbf{r} \in A_\mathrm{e}, \quad (2b)$$

where $\mathbf{H}^{\pm}$ are the fields produced by $\mathbf{M}_{\mathrm{i,e}}$ and the $+/-$ superscripts indicate evaluation just above and below the relevant sections. The field $\mathbf{H}^{\mathrm{sc}}$ is the short-circuited magnetic field, radiated by the impressed sources and the equivalent current $\mathbf{J}$ (existing only over the surface of the PEC load) when the aperture is covered by a PEC surface.

Equations (2) can be cast into coupled IEs by expressing all magnetic fields as superposition integrals (symbol $\otimes$) between the sources and the relevant dyadic GFs:

$$\begin{aligned} &\mathbf{H}^{\mathrm{im}} + \underline{\mathbf{G}}^{\mathrm{C}}_{\mathrm{HJ}} \otimes \mathbf{J} + \underline{\mathbf{G}}^{\mathrm{C}}_{\mathrm{HM}} \otimes \mathbf{M}_\mathrm{i} \\ &\quad = -\underline{\mathbf{G}}^{\mathrm{S}}_{\mathrm{HM}} \otimes \mathbf{M}_\mathrm{i} + \underline{\mathbf{G}}^{\mathrm{M}}_{\mathrm{HM}} \otimes \mathbf{M}_\mathrm{e}, \quad \mathbf{r} \in A_\mathrm{i} \end{aligned} \quad (3a)$$

$$\underline{\mathbf{G}}^{(3)}_{\mathrm{HM}} \otimes \mathbf{M}_\mathrm{e} = -\underline{\mathbf{G}}^{\mathrm{S}}_{\mathrm{HM}} \otimes \mathbf{M}_\mathrm{e} + \underline{\mathbf{G}}^{\mathrm{M}}_{\mathrm{HM}} \otimes \mathbf{M}_\mathrm{i}, \mathbf{r} \in A_\mathrm{e} \quad (3b)$$

where the cross product with $\mathbf{u}_z$ is suppressed throughout. The magnetic field $\mathbf{H}^{\mathrm{im}}$ is that inside the closed cavity due to the impressed dipole sources only (expressed as a suitable combination of components of HM-/HJ-type dyadic GFs of the cavity $\underline{\mathbf{G}}^{\mathrm{C}}_{\mathrm{HM}}$ and $\mathbf{G}^{\mathrm{C}}_{\mathrm{HJ}}$), while $\underline{\mathbf{G}}^{\mathrm{M}}_{\mathrm{HM}}$ and $\underline{\mathbf{G}}^{\mathrm{S}}_{\mathrm{HM}}$ are the GFs of region 2 (i.e., $\underline{\mathbf{G}}^{(2)}_{\mathrm{HM}}$) when observation and source point lie on the opposite and same surface, respectively. Finally, $\underline{\mathbf{G}}^{(3)}_{\mathrm{HM}}$ is the dyadic GF of the external region.

The above formulation requires the evaluation of the GFs in (3); the $\underline{\mathbf{G}}^{(3)}_{\mathrm{HM}}$ GF is not available, neither is the $\underline{\mathbf{G}}^{(2)}_{\mathrm{HM}}$ GF of the closed aperture, except for simple shapes (e.g., rectangular). However, some approximations (discussed next) can be made which allow for a simple solution of the problem without affecting the overall accuracy.

The third equation is obtained by enforcing the EFIE on the surface S of the PEC load inside the enclosure, i.e.,

$$\mathbf{u}_n \times \left(\underline{\mathbf{G}}^{\mathrm{C}}_{\mathrm{EM}} \otimes \mathbf{M}_\mathrm{i} + \underline{\mathbf{G}}^{\mathrm{C}}_{\mathrm{EJ}} \otimes \mathbf{J} \right) = \mathbf{0} \quad \text{on } S, \quad (4)$$

where $\mathbf{u}_n$ indicates the unit vector normal to S and the electric fields have been expressed as superposition integrals between the equivalent magnetic/electric currents and the EM-type/EJ-type dyadic GFs of the cavity $\underline{\mathbf{G}}^{\mathrm{C}}_{\mathrm{EM}}$ and $\underline{\mathbf{G}}^{\mathrm{C}}_{\mathrm{EJ}}$, respectively. Equations (3)-(4) form a set of coupled IEs which, once solved in the unknowns $\mathbf{M}_{\mathrm{i,e}}$ and $\mathbf{J}$, allows for the computation of the EM field inside and outside the enclosure.

IV. NUMERICAL TOOLS

Several approximations can be made together with a clever use of acceleration and interpolation techniques to speed up the computation of all required quantities for the solution of the problem. The most important and somewhat crude and limiting assumption is the following: the enclosure wall containing the aperture is extended to infinity, so that region 3 coincides with the half-space $z > l_z + t$ and the GF of the outer region $\underline{\mathbf{G}}^{(3)}_{\mathrm{HM}}$ can be substituted with twice the free-space GF $\underline{\mathbf{G}}^{\mathrm{fs}}_{\mathrm{HM}}$ (which is known in a simple closed form). As shown in [11] for empty enclosures excited by an impinging uniform plane wave, this approximation leads to an error on the calculated SE_E smaller than 2 dB, regardless of the aperture position. The main drawback of such an approximation is that the radiated field can be evaluated only inside the enclosure and in the half-space beyond the aperture. However, the field outside the enclosure is expected to be maximum right in such an half-space, which thus constitutes the critical region for SE evaluations (as will be discussed in detail in the numerical results). On the other hand, the appealing of such an approximation is enormous, since otherwise the solution of the problem would require the discretization of all the enclosure walls thus introducing an unacceptable number of unknowns.

It should be noted that for vanishing thickness t the formulation in (3) is unstable, since both the GFs $\underline{\mathbf{G}}^{\mathrm{M}}_{\mathrm{HM}}$ and $\underline{\mathbf{G}}^{\mathrm{S}}_{\mathrm{HM}}$ diverge. As first shown in [16], an alternative and robust representation can be obtained by introducing the auxiliary variables $\mathbf{M}_\Sigma = (\mathbf{M}_\mathrm{e} + \mathbf{M}_\mathrm{i})/2$ and $\mathbf{M}_\Delta = (\mathbf{M}_\mathrm{e} - \mathbf{M}_\mathrm{i})/2$ and the GFs $\underline{\mathbf{G}}^{\Sigma}_{\mathrm{HM}} = \underline{\mathbf{G}}^{\mathrm{S}}_{\mathrm{HM}} + \underline{\mathbf{G}}^{\mathrm{M}}_{\mathrm{HM}}$ and $\underline{\mathbf{G}}^{\Delta}_{\mathrm{HM}} = \underline{\mathbf{G}}^{\mathrm{S}}_{\mathrm{HM}} - \underline{\mathbf{G}}^{\mathrm{M}}_{\mathrm{HM}}$ so that (3) can equivalently be written as

$$\underline{\mathbf{G}}_{\mathrm{HJ}}^{\mathrm{C}} \otimes \mathbf{J} + \left(\underline{\mathbf{G}}_{\mathrm{HM}}^{\mathrm{C}} + 2\underline{\mathbf{G}}_{\mathrm{HM}}^{\Delta} + 2\underline{\mathbf{G}}_{\mathrm{HM}}^{\mathrm{fs}}\right) \otimes \mathbf{M}_{\Sigma} + \left(2\underline{\mathbf{G}}_{\mathrm{HM}}^{\mathrm{fs}} - \underline{\mathbf{G}}_{\mathrm{HM}}^{\mathrm{C}}\right) \otimes \mathbf{M}_{\Delta} = -\mathbf{H}^{\mathrm{im}} \quad (5)$$

$$\left(\underline{\mathbf{G}}_{\mathrm{HM}}^{\Delta} + 2\underline{\mathbf{G}}_{\mathrm{HM}}^{\mathrm{fs}}\right) \otimes \mathbf{M}_{\Sigma} + \left(\underline{\mathbf{G}}_{\mathrm{HM}}^{\Sigma} + 2\underline{\mathbf{G}}_{\mathrm{HM}}^{\mathrm{fs}}\right) \otimes \mathbf{M}_{\Delta} = \mathbf{0}$$

which will be discussed next.

A. Thin Apertures

For very thin walls, the case of a zero-thickness aperture can be considered. In such a case the surfaces A_{e} and A_{i} coincide with the unique surface A, only one equivalent magnetic current $\mathbf{M}$ is introduced, and (3)-(4) actually reduce to *two* coupled equations

$$\mathbf{H}^{\mathrm{im}} + \underline{\mathbf{G}}_{\mathrm{HJ}}^{\mathrm{C}} \otimes \mathbf{J} + \underline{\mathbf{G}}_{\mathrm{HM}}^{\mathrm{C}} \otimes \mathbf{M} = -2\underline{\mathbf{G}}_{\mathrm{HM}}^{\mathrm{fs}} \otimes \mathbf{M}, \quad \mathbf{r} \in A \quad (6)$$

$$\mathbf{u}_n \times \left(\underline{\mathbf{G}}_{\mathrm{EM}}^{\mathrm{C}} \otimes \mathbf{M} + \underline{\mathbf{G}}_{\mathrm{EJ}}^{\mathrm{C}} \otimes \mathbf{J}\right) = \mathbf{0} \quad \text{on } S.$$

B. Thick Apertures

As already mentioned above, for thick apertures the system consists of *three* coupled equations. However, for not too large thicknesses, one can assume $\mathbf{M}_{\Delta} = \mathbf{0}$; as shown in [11] for the case of impinging plane waves (and based on the theory developed in [16]), the two coupled equations (5) thus reduce to the *unique* equation

$$\underline{\mathbf{G}}_{\mathrm{HJ}}^{\mathrm{C}} \otimes \mathbf{J} + \left(\underline{\mathbf{G}}_{\mathrm{HM}}^{\mathrm{C}} + 2\underline{\mathbf{G}}_{\mathrm{HM}}^{\Delta} + 2\underline{\mathbf{G}}_{\mathrm{HM}}^{\mathrm{fs}}\right) \otimes \mathbf{M}_{\Sigma} = -\mathbf{H}^{\mathrm{im}} \quad (7)$$

which is formally the same as the first of (6) for the zero-thickness case except for the perturbation term $\underline{\mathbf{G}}_{\mathrm{HM}}^{\Delta}$ which accounts for the finite thickness. As shown in [16], an approximate general expression for $\underline{\mathbf{G}}_{\mathrm{HM}}^{\Delta}$ GF can be obtained by considering the short-circuited cavity as a parallel-plate waveguide; such an expression is available in a simple closed form in the spectral domain and its calculation in the spatial domain requires only the evaluation of a Sommerfeld integral (for details, see [11]).

C. Use of Different Basis Functions for Rectangular Apertures

To discretize (2) and (3), the unknowns (equivalent electric and magnetic currents) need to be expanded through a suitable complete set of vector basis functions (BFs). In order to identify the most convenient representation, several BFs have been tested to represent the equivalent magnetic current on the surface of the aperture and the electric current on the surfaces of the interior conductors.

First, classical Rao-Wilton-Glisson (RWG) rooftop functions [17] have been used: the aperture and the surfaces of the interior conductors have been discretized through nonoverlapping triangles and the unknown current densities $\mathbf{M}$ (or $\mathbf{M}_{\Delta}$) and $\mathbf{J}$ have been expanded in RWG functions as

$$\mathbf{M}(\mathbf{r}) = \sum_{i=1}^{N} a_i^{\mathrm{M}} \boldsymbol{\Lambda}_i(\mathbf{r}), \quad \mathbf{J}(\mathbf{r}) = \sum_{i=1}^{N} a_i^{\mathrm{J}} \boldsymbol{\Lambda}_i(\mathbf{r}), \quad (8)$$

where a_i^{M} and a_i^{J} are unknown complex amplitudes. In the case of thick apertures, when the two surfaces A_{i} and A_{e} have the same shape (which is common in practical cases), the magnetic currents on both the interfaces should share the same mesh to make easier the computation of $\mathbf{M}_{\Sigma}$ and $\mathbf{M}_{\Delta}$.

Alternatively to RWG BFs, in order to achieve a better accuracy, first-order triangular patch (LL) BFs [18] have also been used. In this case, two BFs are associated with each interior edge i of the mesh ($i = 1, \ldots, N_E$) and they are defined on two adjacent triangles T_i^+ and T_i^-, uniquely identified by such i-th edge. These BFs can be expressed as

$$\boldsymbol{\Lambda}_i^1 = \begin{cases} \dfrac{\ell_i}{2A_i^+} \xi_{i+1} \mathbf{l}_{i-1} & \text{if } \mathbf{r} \in T_i^+ \\ \dfrac{\ell_i}{2A_i^-} \xi_{i-1} \mathbf{l}_{i+1} & \text{if } \mathbf{r} \in T_i^- \\ \mathbf{0} & \text{otherwise} \end{cases}$$

$$\boldsymbol{\Lambda}_i^2 = \begin{cases} \dfrac{\ell_i}{2A_i^+} \xi_{i-1} \mathbf{l}_{i+1} & \text{if } \mathbf{r} \in T_i^+ \\ \dfrac{\ell_i}{2A_i^-} \xi_{i+1} \mathbf{l}_{i-1} & \text{if } \mathbf{r} \in T_i^- \\ \mathbf{0} & \text{otherwise} \end{cases} \quad (9)$$

where ℓ_i is the length of the i-th edge, $A_i^{\pm}$ are the areas of the surface triangular patches, ξ_i are the area coordinates, and $\mathbf{l}_i$ is the vector associated

with the edge i. Following the notation used in [19], these BFs provide a linear normal-linear tangent (LN/LT) approximation of the current.

Adding two second-order BFs local to each triangle j ($j=1,...,N_T$) as suggested in [19], it is also possible to obtain a quadratic tangent (LN/QT) approximation along the edges. However, intense testing has demonstrated that the coefficients of these BFs are always two orders of magnitude smaller than the coefficients of the six linear functions, thus not providing a substantial improvement in the modeling of the current.

As concerns the singularities, the GFs in the three regions show a singularity $1/R$ as the observation point approaches the source; in the proposed approach, such a singularity is extracted and analytical formulas [20] are used for the correct integration of the static 3-D GF times the linear vector BFs on source triangles. Classical Gaussian quadrature rules are then used to compute all the remaining source and testing integrals [21].

Finally, entire-domain (ED) BFs have also been used to represent the magnetic current on rectangular apertures. In fact, the use of ED BFs, although restricted to simple geometries, is appealing because it allows for incorporating the possible diverging behavior of the current along the aperture edges and for significantly reducing the size of the MoM matrix. Using ED BFs, the equivalent magnetic current is expressed as

$$M_x = \sqrt{\frac{1-u^2}{1+v^2}} \sum_{m=0}^{M} \sum_{n=0}^{N} M_{0x}^{mn} U_m(u) T_n(v)$$
$$M_y = \sqrt{\frac{1-v^2}{1+u^2}} \sum_{m=0}^{M} \sum_{n=0}^{N} M_{0y}^{mn} U_m(v) T_n(u) \qquad (10)$$

where $M_{0x,y}^{mn}$ are unknown coefficients and $U_n(\cdot)$ and $T_n(\cdot)$ are the n-th order Chebyshev polynomial of first and second kind, respectively. The normalized variables $u=(2x-\ell_x)/\ell_x$ and $v=(2y-\ell_y)/\ell_y$ have been introduced to define the polynomials over the interval $[-1,+1]$ where they are orthogonal. Physically, the equivalent magnetic current components display an inverse square-root singularity at the edges tangential to the direction of the current, while they vanish at the edges normal to such a direction. This behavior is explicitly enforced in the functions in (10) so that they are expected to converge more rapidly to the exact solution. As concerns integration, numerical adaptive formulas have been used to carry out both the source and testing integrals.

It is worth mentioning that the singular behavior at the edges parallel to the direction of the magnetic current could also be enforced over a triangular mesh recurring to special singular RWG functions [22], but with an additional increase of preprocessing and computational efforts. (It should also be noted that in the presence of thick apertures the degree of singularity at the edges is different and another set of ED BFs, involving Gegenbauer polynomials, should be used.)

D. Acceleration of Green's Functions Calculation

Equations (2)-(3) can efficiently be solved by means of the MoM technique (with Galerkin's method) once they have been recast in a mixed-potential form (which is preferred because of the lower-order singularity in the integral kernel) [23]. Introducing the auxiliary potentials $\mathbf{A}$, V, $\mathbf{F}$, and W, the convolution terms can be expressed in terms of potential GFs $\underline{\mathbf{G}}_{A,F}$ and $G_{V,W}$ which, for the free-space case, are known in a simple closed form [1].

From a numerical point of view, a fast computation of the cavity GFs is required to make the proposed integral procedure an efficient technique alternative to classical full-wave methods. The four enclosure GFs are the two dyadic potential $\underline{\mathbf{G}}_{A,F}^{\mathrm{C}}$ (which are diagonal) and the two scalar potential $G_{V,W}^{\mathrm{C}}$. As is well known, the evaluation of the GFs of a rectangular cavity with PEC walls is a daunting task: two classical representations exist, the image and the modal representations, which are both very slowly converging. An efficient numerical acceleration scheme (based on the Ewald representation) is thus adopted, for which the GFs are expressed as a sum of two Gaussian fast-decaying convergent series which depend on the splitting parameter E [24]. The choice of the optimum E plays a crucial role in determining the rapidly-converging character of the series (which actually are multi-

index series and require a clever choice of the strategy used for their numerical summation); several useful details about these issues are given in [25]. Finally, the curls of the GFs can also be computed efficiently in a similar way: the relevant expressions can be found in [26].

E. Interpolation of the Enclosure Green's Function

To further speed-up the computation of all involved GFs, an interpolation technique has been developed in [26], extending the polynomial modeling previously presented in [27].

As concerns the four enclosure GFs, they can be interpolated by means of a triple series of Chebyshev polynomials of the first kind as reported in [26], after extracting their singularities and the singularities in their first derivatives. However, with respect to [26] where odd and even Chebyshev polynomials were used, here we used only even polynomials (this is obtained by interpolating the function $\tilde{D}_q / q$ defined in [26] instead of $\tilde{D}_q$).

The fast computation of the coefficients of the resulting Chebyshev series is a key step to ensure the efficiency of the interpolation. This can be obtained by means of a clever application of the 3-D Fast Cosine Fourier Transform, while the evaluation of the series can be performed by applying the Clenshaw algorithm (for details, see [26],[27]).

V. NUMERICAL RESULTS

A. Choice of the Basis Functions

If not otherwise specified, in all the numerical results presented next, a rectangular $l_x \times l_y \times l_z$ metallic enclosure having a rectangular $a_x \times a_y$ aperture placed in the middle of the wall in the $z = l_z$ plane is considered. The structure is excited by a y-oriented electric dipole placed in the middle of the cavity and the observation point for SE evaluations is located along an axis parallel to z, passing through the aperture center, and at a distance d from it.

A first interesting investigation concerns the determination of the best set of BFs for an accurate SE_E computation. Three different sets have been presented in Section IV.C and all of them have been tested in order to point out their advantages or drawbacks. A specific case is presented in Fig. 3, although the conclusions are general; an empty rectangular metallic enclosure with dimensions $l_x = l_z = 30$ cm and $l_y = 12$ cm has been considered, having a zero-thickness aperture with $a_x = 15$ cm and $a_y = 4$ cm, operating at the frequency $f = 1.5$ GHz. In Fig. 3, the behavior of the amplitude $M = |\mathbf{M}|$ is reported as a function of the observation point over the aperture for RWG BFs (a), LL BFs (b), and ED BFs (c).

It can be observed that, keeping a reasonable number of BFs, ED BFs provide the most accurate representation of the current, which is instead poor in the case of RWG BFs. A smoother curve is obtained through LL BFs, but at the cost of a double number of BFs (compared with RWG BFs with the same mesh). However, when dealing with moderate-size problems, the use of LL BFs significantly improves the accuracy of the solution with the same number of unknowns (i.e., using less triangles) and provides a faster convergence. Despite of these differences, the results obtained for the radiated electric field are *undistinguishable*. In conclusion, ED BFs furnish the most convenient numerical representation because a very small number is required, which entails a smaller MoM matrix size and a smaller number of integrations. On the other hand, if apertures of noncanonical shape are considered, the use of RWG basis functions (about 24 per wavelength) is sufficient to obtain accurate results for the radiated field.

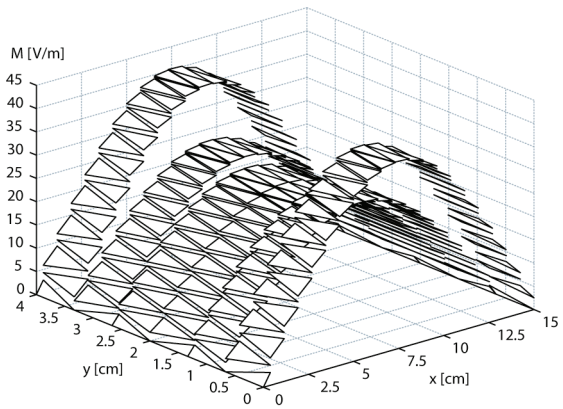

(a)

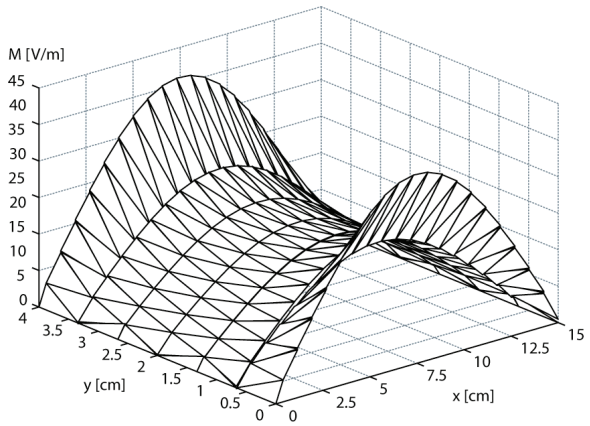

(b)

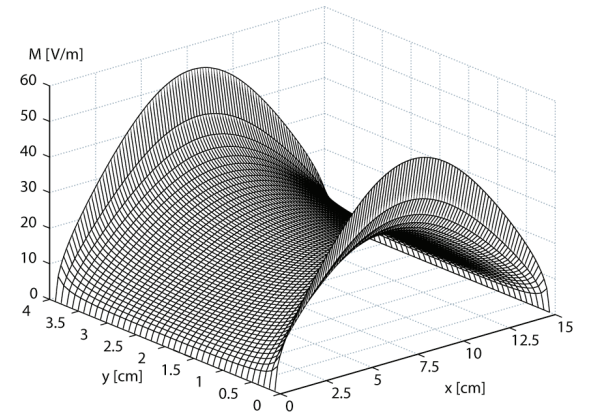

(c)

Fig. 3. Modeling of the equivalent magnetic current using different BFs: RWG (a), LL (b), and ED BFs (c). Parameters are in the text.

B. Thin and Thick Apertures

After testing the use of different types of BFs, we focus on the SE evaluation. A rectangular metallic enclosure with dimensions $l_x = l_y = l_z = 15$ cm has been considered, having aperture dimensions $a_x = 10$ cm and $a_y = 0.5$ cm (i.e., a narrow slot). In Fig. 4, the electric shielding effectiveness SE_E is reported as a function of frequency for an aperture with zero thickness ($t = 0$ mm) and for a thick aperture with $t = 5$ mm. The observation point is located at a distance $d = 20$ cm (i.e., $d = \lambda_0$ at $f = 1.5$ GHz). It can be observed that, as in the case of plane-wave illumination [11], in the case of long slots the finite thickness of the aperture increases the value of the SE_E also by several dB, especially in the low-frequency range. (It should be noted that the enclosure presents resonant frequencies at $f =$ 1.41, 1.73, 2.23, 2.45, 2.83, and 3 GHz, but only few of them are observed in Fig. 4, since for symmetry properties some modes are not excited by the source [1].)

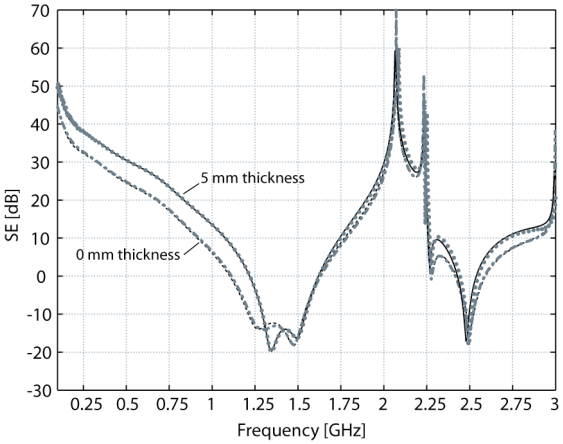

Fig. 4. Electric shielding effectiveness SE_E obtained through the proposed approach (solid line) and CST (dotted line) as a function of frequency for a thin and a thick aperture. Parameters are in the text.

In order to check the accuracy of the proposed approach, our results (solid lines) have been compared with those obtained through the commercial software CST Microwave Studio (based on the Finite Integration Technique in the time domain, dotted lines) and the agreement is excellent. However, even with the use of two planes of symmetry, CST requires a very long simulation time (a mesh with 71300 cells has been used, ensuring 20 cells for wavelength at 3 GHz). To accelerate the simulation, an auto-regressive filter could be used for calculating the frequency spectra without waiting for the probe time signal to reach the steady state, but the accuracy of the results strongly depends on the filter settings, which are very case sensitive.

As explained at the beginning of Section IV, a fundamental approximation of the proposed MoM approach consists in the replacement of the cavity wall containing the aperture with an infinite PEC plane. In the previous results it has been shown that such an approximation does not affect the accuracy of the formulation, at least for points located along the axis parallel to z and passing through the center of the aperture and in the

middle of the enclosure. However, the proposed formulation will certainly fail in evaluating the SE_E for points outside the enclosure and located in the half-space $z < l_z$ (since for the above-mentioned approximation the proposed approach gives a null field in such points). However, this is not a critical drawback since, by trivial considerations, the largest value of the electric field radiated by the dipoles is expected to be found in the half-space $z > l_z$. In any case, it would be interesting to know the limits of the region within which the proposed approach gives accurate results. For this reason, in Fig. 5 the same structure as in Fig. 3 is considered and the electric-field value (in dBV/m) is reported as a function of the angle θ (measured from the axis z with the origin placed at the center of the aperture) on the xz (a) and yz (b) planes, respectively, for different distances ($d =$ 5, 10, 20 cm) from the aperture center at the operating frequency $f = 1.5$ GHz. The results obtained through the proposed approach (solid lines) are compared with the full-wave results obtained through CST (dotted lines) and several remarks can be made.

First, as expected, the electric-field values are lower and lower by increasing the distance from the aperture (in Fig. 5 such values are normalized with respect to the maximum value present in the $d = 5$-cm case).

Let us consider now the xz plane (Fig. 5(a)); the length of the cavity wall along x is $l_x = 30$ cm, while the aperture dimension is $a_x = 10$ cm so that the curves corresponding to $d = 5$ cm and $d = 10$ cm end at $\theta = \pm 90^\circ$ (for which the observation point lies on the cavity wall), whereas the curve corresponding to $d = 20$ cm extends in the $z < l_z$ half-space. Interestingly, the pattern is almost isotropic in the very near-field region over the whole angular range (for $d = 5$ cm) or in a very wide angular range (for $d = 10$ cm and $d = 20$ cm). In any case, a very good agreement is always obtained in the $z > l_z$ half-space, while the electric-field values for $z < l_z$ when $d = 20$ cm are completely negligible (about 25 dB lower than the maximum value occurring at $\theta = 0^\circ$).

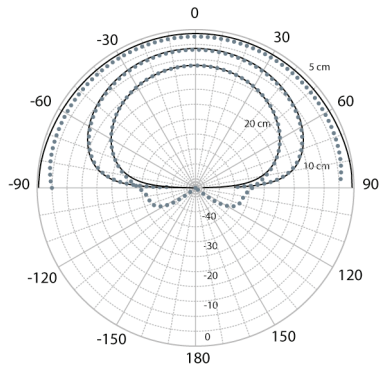

(a)

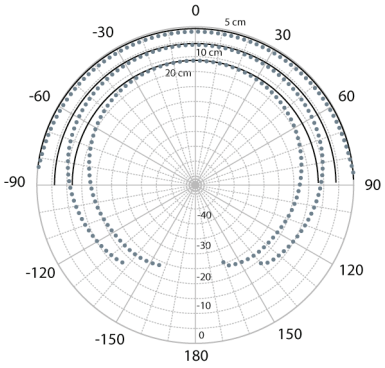

(b)

Fig. 5. Normalized electric-field amplitudes (in dBV/m) obtained through the proposed approach (solid line) and CST (dotted line) for different values of d in the xz (a) and yz plane (b). Parameters are in the text.

As concerns the yz plane (Fig. 5(b)), it results $l_y = 12$ cm and $a_y = 4$ cm; in this case only the curve corresponding to $d = 5$ cm ends at $\theta = \pm 90^\circ$. As in the xz plane, the pattern is almost isotropic over the whole angular range and an excellent agreement is obtained between the results of the proposed approach and those of CST. The curves corresponding to $d = 10$ cm and $d = 20$ cm extend in the $z < l_z$ lower half-space; they are nearly isotropic over the whole angular range for $z > l_z$ and a very good agreement is obtained between our formulation and the full-wave results (the maximum error is about 5 dB and obviously occurs over the plane $z = l_z$). In any case, the electric-field values for $z < l_z$ are lower than those for $z > l_z$ by about 5 – 10 dB, thus

confirming that the maximum radiation is obtained in the half-space above the aperture.

C. Loaded Enclosures

It is then interesting to study the effects of possible PEC loadings placed inside the enclosure. The same structure as in Fig. 5 (with a zero-thickness aperture) has been considered but loaded with a PEC plate parallel to the yz plane, with dimensions $d_y = 8$ cm and $d_z = 20$ cm and with its center located at (7, 6, 12) cm. (It should be noted that if the plates are connected to the cavity walls, suitable local basis functions defined on the triangles at the edges between the plates and the cavity walls have to be used, as done in [26].)

First, the SE_E of the empty enclosure has been studied as a function of frequency for $d = 20$ cm. The relevant results are reported in Fig. 6(a) (solid line) and they are compared with those obtained with both CST (dotted line) and FEKO (based on a frequency domain MoM, dashed line), showing an excellent agreement.

In Fig. 6(b), the SE_E of the loaded enclosure is reported, with the observation point as in Fig. 6(a). In this case, the calculation of the SE_E has been performed through the definition (1), where $\mathbf{E}^{\mathrm{inc}}(\mathbf{r})$ is assumed as the electric field radiated by the electric dipole *in the presence of the plate* and in the absence of the enclosure. Again, the results obtained with the proposed approach are in excellent agreement with those obtained with both CST and FEKO. However, FEKO uses 3504 triangles (10 triangles per wavelength) and requires about 2 hours to compute 601 frequency points (on a 3 GHz Intel Quad Core CPU), while CST uses 75800 cells and requires about 3 hours (with parallelization on four threads) to extinguish the transient inside the enclosure with an accuracy of -60 dB (in this case, due to the presence of the loading, only one plane of symmetry can be used). The proposed method, with 376 overall unknowns, requires just 72 minutes to compute 601 frequency points, providing a dramatic acceleration without affecting the accuracy of the results. A comparison between Fig. 6(a) and (b) also reveals that the SE_E is seriously affected by the presence of the PEC plate, especially in the high-frequency range.

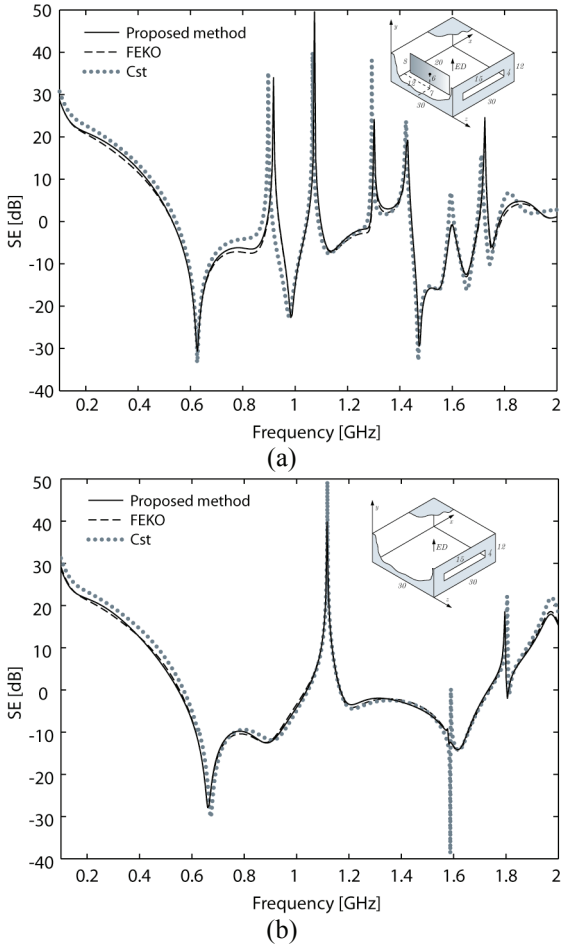

Fig. 6. SE_E obtained through the proposed approach (solid line), CST (dotted line), and FEKO (dashed line) as a function of frequency. Empty enclosure (a); loaded enclosure (b). Parameters are in the text.

D. Different Dipole Sources and Orientations

Finally, different types and orientations of the dipole sources have been considered. In fact, while an electric dipole represents a short linear antenna, a magnetic dipole may represent a small loop antenna lying on the plane orthogonal to the dipole direction. The SE_E has been calculated as a function of frequency for the same structure as in Fig. 4 at a distance $d = 20$ cm from the aperture.

In Fig. 7(a), the effects of electric dipole sources placed in the center of the enclosure and directed along the main axes (x, y, z) are reported. It can be seen that the worst case is represented by a y-oriented dipole (i.e., parallel to the shortest side of the aperture), which gives rise to values of

SE_E several dB lower than those corresponding to the other dipole orientations. The latter orientations present critical values of the SE_E only in correspondence of the resonant frequencies of the metallic cavity.

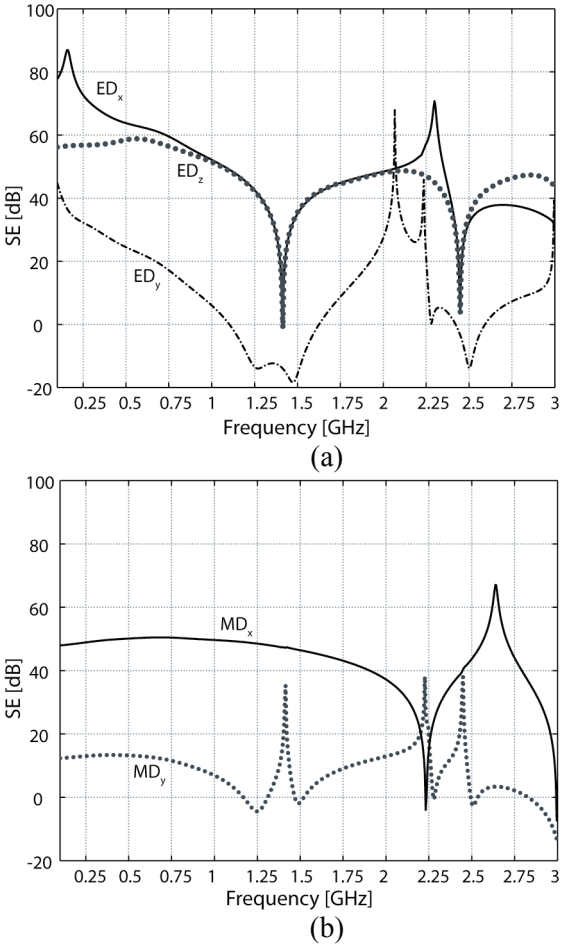

Fig. 7. SE_E obtained through the proposed approach as a function of frequency for different kind of sources and orientations: electric dipole (a) and magnetic dipole (b). Parameters are in the text.

In Fig. 7(b), the SE_E due to magnetic dipoles placed in the center of the enclosure and directed along the main axes (x, y, z) is shown. It can be seen that also for this excitation the worst case is represented by a y-oriented dipole (i.e., parallel to the shortest side of the aperture). It should be noted that no curve is reported corresponding to the z-oriented magnetic dipole: in fact, in such a case the planes containing the dipole and orthogonal to the xy plane are equivalent to PEC planes (by symmetry), so that at the observation point (which lies along the intersection between such planes) the electric field is null [1].

VI. CONCLUSIONS

This work has presented a detailed study of the shielding effectiveness of rectangular metallic enclosures having thin or thick apertures, possibly loaded with conducting bodies and the problem of a finite-source excitation (i.e., an arbitrarily oriented electric or magnetic dipole placed inside the cavity) has been addressed, instead of the more conventional plane-wave excitation; in fact, the dipoles may represent practical sources such as short-linear or small-loop antennas. An efficient Method-of-Moment formulation has been developed which overcomes typical difficulties of the classical approach through the use of acceleration techniques for the computation of the dyadic enclosure Green's function, interpolation schemes, different sets of basis functions modeling the apertures, and approximations which dramatically simplify the problem. Such approximations have been critically discussed and it has been shown how they still allow for maintaining a high level of accuracy in the problem solution. The efficiency and the accuracy of the proposed approach has been fully validated by means of comparisons with results obtained through independent full-wave software, thus showing the validity and the appealing of the method in solving this classical electromagnetic problem.

REFERENCES

[1] S. Celozzi, R. Araneo, and G. Lovat, *Electromagnetic Shielding*, Wiley-IEEE, Hoboken, 2008.

[2] W. Wallyn, D. De Zutter, and H. Rogier, "Prediction of the shielding and resonant behavior of multisection enclosures based on magnetic current modeling," *IEEE Trans. Electromagn. Compat.*, vol. 44, no. 1, pp. 130–138, Feb. 2002.

[3] F. Olyslager, E. Laermans, D. De Zutter, S. Criel, R. De Smedt, N., Lietaert, and A. De Clercq, "Numerical and experimental study of the shielding effectiveness of a metallic enclosure," *IEEE Trans. Electromagn. Compat.*, vol. 41, no. 3, pp. 202–213, Aug. 1999.

[4] M. P. Robinson, T. M. Benson, C. Christopoulos, J. F. Dawson, M. D. Ganley, A. C. Marvin, S. J. Porter, and D. W. P. Thomas, "Analytical formulation for the shielding effectiveness of enclosures with apertures," *IEEE Trans. Electromagn. Compat*., vol. 40, no. 3, pp. 240–248, Aug. 1998.

[5] R. Azaro, S. Caorsi, M. Donelli, and G. L. Gragnani, "A circuital approach to evaluating the electromagnetic field on rectangular apertures backed by rectangular cavities," *IEEE Trans. Microw. Theory Tech*., vol. 50, no. 10, pp. 2259–2264, Oct. 2002.

[6] T. Konefal, J. F. Dawson, A. Marvin, M. P. Robinson, and S. J. Porter, "A fast multiple mode intermediate level circuit model for the prediction of shielding effectiveness of a rectangular box containing a rectangular aperture," *IEEE Trans. Electromagn. Compat*., vol. 47, no. 4, pp. 678–691, Nov. 2006.

[7] S. Benhassine, L. Pinchon, and W. Tabbara, "An efficient finite-element time-domain method for the analysis of the coupling between wave and shielded enclosure," *IEEE Trans. Magn.*, vol. 38, no. 2, pp. 709–712, Feb. 2002.

[8] H. H. Park and H. J. Eom, "Electromagnetic penetration into a rectangular cavity with multiple rectangular apertures in a conducting plane," *IEEE Trans. Electromagn. Compat*., vol. 42, no. 3, pp. 303–307, Aug. 2000.

[9] G. Cerri, R. De Leo, and V. M. Primiani, "Theoretical and experimental evaluation of the electromagnetic radiation from apertures in shielded enclosures," *IEEE Trans. Electromagn. Compat.*, vol. 34, no. 4, pp. 423–432, Nov. 1992.

[10] V. Rajamani, C. F. Bunting, M. D. Deshpande, and Z. A. Khan, "Validation of Modal/MoM in shielding effectiveness studies of rectangular enclosures with apertures," *IEEE Trans. Electromagn. Compat.*, vol. 48, no. 2, pp. 348–352, May 2006.

[11] R. Araneo and G. Lovat, "An efficient MoM formulation for the evaluation of the shielding effectiveness of rectangular enclosures with thin and thick apertures," *IEEE Trans. Electromagn. Compat.*, vol. 50, no. 2, pp. 294–304, May 2008.

[12] M. Li, J. Nuebel, J. L. Drewniak, T. H. Hubing, R. E. DuBroff, and T. P. Van Doren, "EMI from cavity modes of shielding enclosures – FDTD modeling and measurements," *IEEE Trans. Electromagn. Compat.*, vol. 42, no.1, pp. 29–38, Jan. 2000.

[13] S. V. Georgakapoulos, C. R., Birtcher, and C. A. Balanis, "HIRF penetration through apertures: FDTD versus measurements," *IEEE Trans. Electromagn. Compat.*, vol. 43, no. 3, pp. 282–294, Aug. 2001.

[14] C. Jiao, X. Cui, L. Li, and H. Li, "Subcell FDTD analysis of shielding effectiveness of a thin-walled enclosure with an aperture," *IEEE Trans. Magn.*, vol. 42, no. 4, pp. 1075–1078, Apr. 2006.

[15] C. Feng and Z. Shen, "A hybrid FD-MoM technique for predicting shielding effectiveness of metallic enclosures with apertures," *IEEE Trans. Electromagn. Compat.*, vol. 47, no. 3, pp. 456–462, Aug. 2005.

[16] J. R. Mosig, "Scattering by arbitrarily-shaped slots in thick conducting screen: An approximate solution," *IEEE Trans. Antennas Propag.*, vol. 52, no. 8, pp. 2109–2117, Aug. 2004.

[17] S. M. Rao, D. R. Wilton, and A. W. Glisson, "Electromagnetic scattering by surfaces of arbitrary shape," *IEEE Trans. Antennas Propag.*, vol. 30, no. 3, pp. 409–418, Mar. 1982.

[18] L. C. Trintinalia, and H. Ling "First order triangular patch basis functions for electromagnetic scattering analysis," *J. Electromagn. Waves Appl.*, vol. 15, no. 11, pp. 1521–1537, 2001.

[19] A. F. Peterson, S. L. Ray, and R. Mittra, *Computational Methods for Electromagnetics*, IEEE Press, Piscataway, 1998.

[20] R. D. Graglia, "On the numerical integration of the linear shape functions times the 3-D Green's function or its gradient on a plane triangle," *IEEE Trans. Antennas Propag.*, vol. 41, no. 10, pp. 1448–1455, Oct. 2001.

[21] D. A. Dunavant, "High degree efficient symmetrical gaussian quadrature rules for the triangle," *Intern. Journal Num. Meth. Engineering*, vol. 21, pp. 1129–1148, 1985.

[22] J. W. Brown and D. R. Wilton "Singular basis functions and curvilinear triangles in the solution of the electric field integral equation," *IEEE Trans. Antennas Propag.*, vol. 47, no. 2, pp. 347–353, Feb. 2001.

[23] J. R. Mosig, "Integral equation technique," *Numerical techniques for microwave and millimeter wave passive structures*, Wiley, 1989.

[24] M.-J. Park, J. Park, and S. Nam, "Efficient calculation of the Green's function for the rectangular cavity," *IEEE Microwave Guided Wave Lett.*, vol. 8, no. 3, pp. 124–126, Mar. 1998.

[25] G. Lovat, P. Burghignoli, and R. Araneo, "Efficient evaluation of the three-dimensional periodic Green's function through the Ewald method," *IEEE Trans. Microw. Theory Tech.*, vol. 56, no. 9, pp. 2069–2075, Sep. 2008.

[26] R. Araneo and G. Lovat, "Fast MoM analysis of the shielding effectiveness of rectangular enclosures with apertures, metal plates, and conducting objects," *IEEE Trans. Electromagn. Compat.*, vol. 51, no. 2, pp. 274–283, Feb. 2009.

[27] A. Borij and S. Safavi-Naeni, "Rapid calculation of the Green's function in a rectangular enclosure with application to conductor loaded cavity resonators," *IEEE Trans. Microw. Theory Tech.*, vol. 52, no. 7, pp. 1724–1731, Jul. 2004.

Rodolfo Araneo was born in Rome, Italy, on October 29, 1975. He received the M.S. (*cum laude*) and Ph.D. degrees in electrical engineering from the University of Rome "La Sapienza", Rome, in 1999 and 2002, respectively.

During the master thesis in 1999 he was a Visiting Student at the National Institute of Standards and Technology (NIST) Boulder, CO where he worked on TEM cells and shielding. During the second semester of the year 2000 he was a Visiting Researcher of the Department of Electrical and Computer Engineering of University of Missouri–Rolla (UMR) where he worked on printed circuit boards and finite-difference time-domain techniques.

Dr. Araneo received the Past President's Memorial Awards in 1999 from IEEE EMC Society. His research activity is mainly in the field of electromagnetic compatibility (EMC) and includes numerical and analytical techniques for modelling high-speed printed circuit boards, shielding, and transmission line analysis.

Giampiero Lovat was born in Rome, Italy, on May 31, 1975. He received the Laurea degree (*cum laude*) in electronic engineering and the Ph.D. degree in applied electromagnetics, both from "La Sapienza" University of Rome, Rome, Italy, in 2001 and 2005, respectively.

In 2005, he joined the Electrical Engineering Department of "La Sapienza" University of Rome, where he is currently an Associate Researcher. From January 2004 to July 2004 he was a Visiting Scholar at the University of Houston, Houston, Texas. His present research interests include leaky-wave antennas, general theory and numerical methods for the analysis of periodic structures, electromagnetic theory of complex media, and shielding analysis of enclosures and of planar composite screens.

Dr. Lovat received a Young Scientist Award from the 2005 URSI General Assembly, New Delhi, India.